A Nonorthogonal Higher-Order Wavelet-Oriented FDTD Technique for 3-D Waveguide Structures on Generalized Curvilinear Grids

Nikolaos V. Kantartzis, *Student Member, IEEE*, Thedoros I. Kosmanis, *Student Member, IEEE*, Traianos V. Yioultsis, and Theodoros D. Tsiboukis, *Senior Member, IEEE*

***Abstract*—A generalized higher-order FDTD rendition of the covariant and contravariant vector component theory for the accurate modeling of complex waveguides in 3-D nonorthogonal curvilinear coordinates, is presented in this paper. The novel algorithm, which postulates conventional and nonstandard concepts, embodies a spatially-localized Wavelet-Galerkin formulation in order to efficiently deal with fast field variations in the vicinity of arbitrarily-angled wedges. The proposed method is combined with a pulsed excitation and enhanced unsplit-field PMLs thus, achieving significant accuracy and suppression of all discretization errors with a simultaneous diminishment of computational resources, as indicated by various numerical results.**

***Index Terms*—Curvilinear nonorthogonal coordinates, FDTD methods, higher-order schemes, waveguides, wavelet transforms.**

I. Introduction

WAVEGUIDE structures with arbitrarily-curved cross-section, irregular shape and complex coupling discontinuities, constitute an indispensable class of components in many microwave device applications. The continuously increasing design requirements, render the advanced numerical simulation of these systems an issue of intensive scientific research [1], [2]. The FDTD method has been implemented for the treatment of such devices, however the method's classical restriction to staircase approximations and second-order differencing leads to inadequate discretization and dispersion errors. For instance, the accurate modeling of circular cross-section waveguides or arbitrarily inclined slots by means of the usual Yee cells demands a highly refined mesh. On the other hand, the traditional ways of excitation necessitate the use of long uniform parts and therefore, excessive requirements in memory capacity and CPU time. Various efficient techniques in combination with the FDTD method have been introduced, using conformal mapping [3], generalized lattices [4] and wavelet-based configurations [5], [6], although they do not completely overcome the above shortcomings.

In this paper a new, fully nonorthogonal higher-order FDTD methodology, founded on curvilinear conventional and nonstandard concepts, is introduced for the accurate analysis of complicated 3-D waveguides. By postulating a higher-order covariant/contravariant strategy, the technique implements a self-adaptive compact central difference procedure to treat the inevitably widened spatial stencils. For the simulation of rapidly-varying local field disturbances near conductive wedges, a Wavelet-Galerkin (WG) formulation is developed, attaining advanced geometric versatility and coarse lattices in the vicinity of demanding discontinuities. Furthermore, a pulsed excitation performs remarkable grid savings by enabling the use of enhanced unsplit-field PMLs sufficiently close to any structural discontinuity. Performance verification of the proposed method is accomplished via various microwave device problems with complex cross-sections and coupling slots. Their main goal is the accurate calculation of the cut-off frequencies and the S-parameters.

Manuscript received June 5, 2000.

This work was supported in part by the Greek General Secretariat of Research & Technology (Grant 99ED325).

The authors are with the Department of Electrical and Computer Engineering, Aristotle University of Thessaloniki, GR-54006, Greece (e-mail: tsibukis@vergina.eng.auth.gr).

Publisher Item Identifier S 0018-9464(01)07798-6.

II. Higher-Order Nonorthogonal FDTD Concepts

A. Construction of the Higher-Order Schemes

The essential premises of the new FDTD methodology are the higher-order (HO) finite-difference formulae, conventional or nonstandard, the latter of which approximate the spatial and temporal derivatives via the following operator

$$\mathbf{DS}_u^{nst}[f|_u^t] = \tfrac{11}{12}\,\mathbf{D}_{u,\,\delta u}^{nst}[f|_u^t] + \tfrac{1}{24} \cdot \left(\mathbf{D}_{u,\,3\delta u}^{nst}[f|_u^t] + \frac{f|_{u-\delta u/2}^t - f|_{u-3\delta u/2}^t}{\delta u}\right), \tag{1}$$

where u belongs to the general coordinate system $(u,\,v,\,w)$ and $\mathbf{D}_{u,\,\delta h}^{nst}(\delta h = \delta u,\,3\delta u)$ is the 3-D nonstandard operator, given by

$$\mathbf{D}_{u,\,\delta h}^{nst}[f|_u^t] \equiv \frac{1}{m_k(k\delta h)}\left(q_1\mathbf{d}_{u,\,\delta h}^{(1)}[f|_u^t] + q_2\mathbf{d}_{u,\,\delta h}^{(2)}[f|_u^t] + q_3\mathbf{d}_{u,\,\delta h}^{(3)}[f|_u^t]\right). \tag{2}$$

The $m_k(k\delta h)$ is a correction function (of sinusoidal form) selected to minimize the inevitable error generated by the derivative approximation in (1), as well as to significantly enhance the technique's dispersion and dissipation features. For a precise and consistent simulation of the continuous physical space in terms of its discretized counterpart, the difference operators $\mathbf{d}$ in (2) are expressed by the following forms which completely exploits the geometry of the elementary cell, as shown in Fig. 1,

$$\mathbf{d}_{u,\,\delta h}^{(1)}[f|_{u,\,v,\,w}^t] = f|_{\delta h/2,\,0,\,0}^t - f|_{-\delta h/2,\,0,\,0}^t, \tag{3}$$

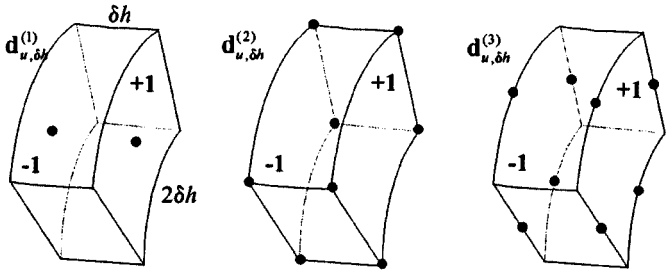

Fig. 1. The curvilinear finite difference operators. The numbers at the cell faces determine the sign of summation.

$$\mathbf{d}^{(2)}_{u,\delta h}[f|^t_{u,v,w}] = \frac{1}{2}\begin{pmatrix} f|^t_{\delta h/2,\delta h,\delta h}+f|^t_{\delta h/2,\delta h,-\delta h}+f|^t_{\delta h/2,-\delta h,\delta h} \\ +f|^t_{\delta h/2,-\delta h,-\delta h}-f|^t_{-\delta h/2,\delta h,\delta h}-f|^t_{-\delta h/2,\delta h,-\delta h} \\ -f|^t_{-\delta h/2,-\delta h,\delta h}-f|^t_{-\delta h/2,-\delta h,-\delta h} \end{pmatrix}, \tag{4}$$

$$\mathbf{d}^{(3)}_{u,\delta h}[f|^t_{u,v,w}] = \frac{1}{4}\begin{pmatrix} f|^t_{\delta h/2,\delta h,0}+f|^t_{\delta h/2,-\delta h,0}+f|^t_{\delta h/2,0,\delta h} \\ +f|^t_{\delta h/2,0,-\delta h}-f|^t_{-\delta h/2,\delta h,0}-f|^t_{-\delta h/2,-\delta h,0} \\ -f|^t_{-\delta h/2,0,\delta h}-f|^t_{-\delta h/2,0,-\delta h} \end{pmatrix}. \tag{5}$$

For brevity, in (3)–(5) only the respective lattice space increments toward the u, v, w directions are indicated (i.e., the notation $-\delta h/2$, 0, δh means $u-\delta h/2$, v, $w+\delta h$). The analogously significant q parameters, mainly responsible for the stable and well-posed profile of the algorithm, are calculated via

$$q_1 = p + s(1-p)/3, \qquad q_2 = s(1-p)/3, \tag{6a}$$

$$q_3 = 1 - p - 2s(1-p)/3, \tag{6b}$$

with

$$s(k) = \frac{pR_A + (1-p)R_B - (\cos k - 1)}{(p-1)(R_A + R_B - 2R_C)}, \tag{7a}$$

$$p(k) = \frac{\cos k_u \cos k_v - \cos k}{1 + \cos k_u \cos k_v - \cos k_u - \cos k_v}, \tag{7b}$$

while the coefficients R_A, R_B and R_C are mathematically described as functions of the wave number components, as

$$R_A = \cos k_u + \cos k_v + \cos k_w - 3, \tag{8a}$$

$$R_B = \cos k_u \cos k_v \cos k_w - 1, \tag{8b}$$

$$R_C = 0.5(\cos k_u \cos k_v + \cos k_u \cos k_w + \cos k_v \cos k_w - 3). \tag{8c}$$

According to the nonstandard regime, temporal discretization receives the subsequent form

$$\mathbf{DT}^{nst}[f|^t_u] = \left(f|^{t+\delta t/2}_u - f|^{t-\delta t/2}_u\right) \Big/ m_\omega(\omega\delta t) - (\delta t^2/24)\,\partial_{ttt} f|^t_u, \tag{9}$$

where ∂_{ttt} denotes third-order time differentiation and $m_\omega(\delta t)$ is the respective correction function. Time integration (except of the leapfrog scheme) is performed by means of the fourth-stage Runge–Kutta integrator, generally given by

$$f|^{n+1}_{i,j,k} = \sum_{m=1}^{M} \frac{(-\delta t \Xi)^m}{m!} \cdot f|^n_{i,j,k}, \tag{10}$$

in which Ξ is the spatial discretization matrix and M the order of the integrator. Being conditionally stable and unaffected by the incorporation of compact operators, as its second-order counterpart, this integrator performs 1.4 times more efficiently than the fourth-order leapfrog one.

Another prominent attribute of the HO curvilinear FDTD schemes is the widened spatial stencil near perfectly conducting interfaces and absorbing walls. To circumvent this difficulty, a general class of self-adaptive compact operators is presented, which guarantees the thorough modeling of complex applications. Specifically, they can be expressed (in central or nonsymmetric version) by the Hermite formula

$$\sum_{pos=-1}^{1} \left(a_{pos} f_{i+pos} + b_{pos} f'_{i+pos} + c_{pos} f''_{i+pos}\right) = 0 \tag{11}$$

where α_i, b_i, c_i are unknown calculable real coefficients.

B. Treatment of the Curvilinear Div–Curl Problem

The strong dependence of every field quantity—involved in the curvilinear form of Maxwell's equations—on the choice of the basis system plays a crucial role in the consistency of the numerical solution, since an improper selection may give rise to Cristoffel symbols, that cannot be accurately computed [7]. To derive a consistent solution of this strenuous div–curl problem, we develop a new algorithm incorporating a fully conservative HO rendition of the covariant/contravariant theory, which considers all metric terms. Its main idea is the use of a Helmholtz-type decomposition that computes the desired electric or magnetic vector via the projection of the curl onto the space of divergence-free vectors [8].

Assuming that the computational domain is described by a general nonorthogonal right-handed curvilinear coordinate system (u, v, w) and that this mapping is smooth enough, any vector $\mathbf{F}$ can be decomposed with respect to the contravariant $\mathbf{a}^1$, $\mathbf{a}^2$, $\mathbf{a}^3$ or the covariant $\mathbf{a}_1$, $\mathbf{a}_2$, $\mathbf{a}_3$ base system. Therefore, the curl of vector $\mathbf{F}$ can be computed as

$$\mathbf{F} = \sum_{i=1}^{3} (\mathbf{a}_i \cdot \mathbf{F})\,\mathbf{a}^i = \sum_{i=1}^{3} f_i\,\mathbf{a}^i = \sum_{i=1}^{3} (\mathbf{a}^i \cdot \mathbf{F})\,\mathbf{a}_i = \sum_{i=1}^{3} f^i\,\mathbf{a}_i. \tag{12}$$

The quantities f^i, f_i denote respectively the contravariant and covariant components of $\mathbf{F}$ which, due to their reciprocity, satisfy the relation $\mathbf{a}_i \cdot \mathbf{a}^j = \delta_{ij}$ (δ_{ij} is the Kronecker's delta). The metrical coefficients of the coordinate system g_{ij}, g^{ij} are defined by $g_{ij} = g_{ji} = \mathbf{a}_i \cdot \mathbf{a}_j$, $g^{ij} = g^{ji} = \mathbf{a}^i \cdot \mathbf{a}^j$, and $g^{1/2} = \mathbf{a}_i \cdot (\mathbf{a}_j \times \mathbf{a}_k)$ with a cyclic permutation of indices i, j, k. Therefore, the curl of vector $\mathbf{F}$ can be computed

$$\nabla \times \mathbf{F} = \frac{1}{\sqrt{g}} \left[\left(\frac{\partial f_3}{\partial v} - \frac{\partial f_2}{\partial w}\right)\mathbf{a}_1 + \left(\frac{\partial f_1}{\partial w} - \frac{\partial f_3}{\partial u}\right)\mathbf{a}_2 + \left(\frac{\partial f_2}{\partial u} - \frac{\partial f_1}{\partial v}\right)\mathbf{a}_3 \right]. \tag{13}$$

Derivative approximation in (13), yields an accurate HO curvilinear FDTD curl operator which is subsequently applied to Maxwell's equations. For illustration, the general matrix form of Ampere's law becomes

$$\left(\mathbf{I}+\tfrac{1}{2}\,\mathbf{A}_t\right)\mathbf{E}_c^{n+1}=\left(\mathbf{I}-\tfrac{1}{2}\,\mathbf{A}_t\right)\mathbf{E}_c^{n}+\mathbf{G}_s\mathbf{D}\mathbf{S}^{nst}\left[\mathbf{H}_c^{n+1/2}\right]. \tag{14}$$

where c denotes the unknown covariant electric components and $\mathbf{A}_t$, $\mathbf{G}_s$ derivative and metric tensor operators, respectively. Thus, the curvilinear div–curl problem which consists of finding a vector field $\mathbf{F}$ assuming that its curl and its divergence are known, is efficiently treated by our method.

Finally, the stability criterion of our method becomes

$$c\delta t \le \frac{3\sin^{-1}(0.7)}{\pi\left(\sum_{l=1}^{3}\sum_{m=1}^{3}\dfrac{g^{lm}}{\delta\zeta^{l}\delta\zeta^{m}}\right)^{1/2}}, \qquad \text{with } \zeta^{l,m}=u,\,v,\,w. \tag{15}$$

III. FDTD–Wavelet-Galerkin Formulation

The novel algorithm also allows accurate treatment of field singularities, such as conductive wedges, since it embodies the spatially-localized FDTD–Wavelet-Galerkin technique [9]. According to the latter, the computational domain is divided into regions of sharp (in the vicinity of the discontinuities) and regions of smooth field transitions (rest of the domain). Each field component in the former area, analyzed by the Wavelet-Galerkin technique, is expanded in a set of Daubechies' scaling functions [10] as

$$F(x,\,y,\,z,\,t)=\sum_{i,\,j,\,k}\sum_{n}F_{ijk}^{n}\varphi_i(x)\varphi_j(y)\varphi_k(z)h_n(t) \tag{16}$$

where the F_{ijk}^{n} terms correspond to any ($x=i\delta x$, $y=j\delta y$, $z=k\delta z$) node of the grid at $t=n\delta t$, $\varphi_\zeta(\xi)$ is an appropriate scaling function, herein selected to be Daubechies', and $h_n(t)$ the Haar scaling function. Substitution of (16) into Maxwell's curl equations and implementation of the Galerkin Weighted Residuals procedure lead to a set of WG equations that are very similar to those of the FDTD method. For example, the 3-D E_z expression (similarly for the others) at $n+1$ time step is

$$E_z|_{i,\,j,\,k}^{n+1}=E_z|_{i,\,j,\,k}^{n}+\sum_{p}\mathrm{r}(p)\frac{\delta t}{\varepsilon_0}\cdot\left(\frac{H_y|_{i+p+0.5,\,j,\,k}^{n+0.5}}{\delta x}-\frac{H_x|_{i,\,j+p+0.5,\,k}^{n+0.5}}{\delta y}\right). \tag{17}$$

In (17), $\mathrm{r}(p)$ are coefficients that depend only on the scaling function selected [9]. On the contrary, the rest of the computational domain, where singularities are absent, is treated by the more convenient, linear FDTD method.

The coexistence of these two efficient techniques at the interface is straightforward, on condition that spatial and temporal increments are equal, an issue that is easily attained. Thus, updates of field components near the interface requires samples from both FDTD and WG areas. Such a treatment causes no inconsistency or instability, avoids unnecessary complications and maintains the enhanced accuracy. Thus, the overall time needed for the new scheme to obtain an accurate solution, is notably decreased compared to the one needed for the pure WG or the standard FDTD methods.

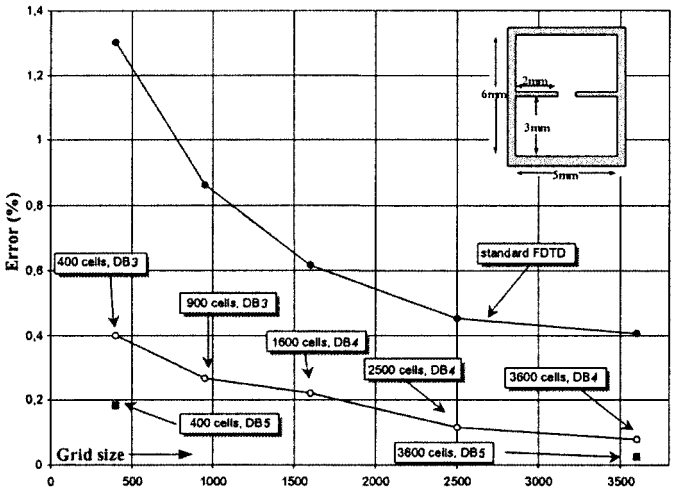

Fig. 2. Variation of the relative error vs grid size. An increase in the number of vanishing moments, N, enhances the solution's accuracy.

Evidently, when the FDTD–WG technique is efficiently combined with the proposed HO method, an even greater reduction of the computational resources—with simultaneous significant suppression of dispersion, dissipation and anisotropy errors—is attained. Particularly, the lattice becomes very coarse without loss of accuracy, since the hybrid scheme allows significant reduction of the grid around the discontinuities and the HO method decreases that of the rest of the domain. This is extremely important in 3-D waveguide structures, which for an accurate analysis, normally require dense grids and very long FDTD simulation procedures.

IV. Numerical Results

The implementation of the proposed technique to diverse 2-D and 3-D waveguide problems where discontinuities occur, verified its merits and enhanced accuracy. It is to be mentioned herein that the excitation of the 3-D structures is performed by a pulsed modulated process which imposes the source plane several cells away from the ABC's plane in order to fully separate incident and reflected fields. Considering a distance of d_c cells, E_v is expressed as

$$E_{v+d_c}^{n+1}=\mathrm{FDTD}\qquad update+L(u,\,v)\sum_{s=1}^{N}\sin(2\pi f_s t-\beta_s w), \tag{18}$$

where $L(u,\,v)$ represents the pulse's spatial profile.

The first application involves a 2-D structure (embedded picture in Fig. 2), the TM (Fig. 2) and TE (Fig. 3) mode resonant frequencies of which are computed via several FDTD and FDTD–WG formulations. The essential reduction of the grid size and hence of the overall computational time is obvious as compared to the FDTD method, given a constant error level. Furthermore, indicative time reduction factors (rf) clearly reveal the decrease of the computational resources.

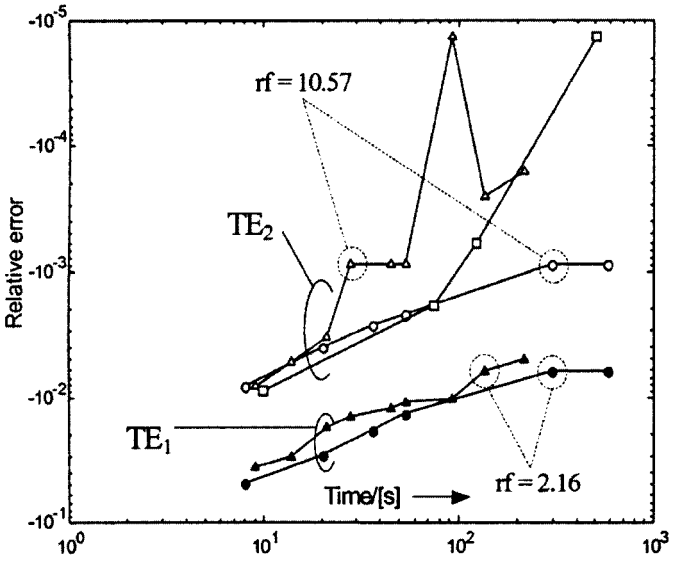

Fig. 3. Error comparison of resonant frequencies as a function of time: FDTD (circles), DB2 (triangles), DB4 (squares).

TABLE I
RELATIVE ERROR FOR THE ANGLED-WEDGE CASE

Technique	TE_1	TE_2
Hybrid (DB*3*, 50×50)	-0.533 %	-0.089 %
Hybrid (DB*3*, 100×100)	-0.0582 %	-0.014 %
FDTD (50×50)	-0.567 %	-0.126 %
FDTD (150×150)	-0.063 %	-0.033 %

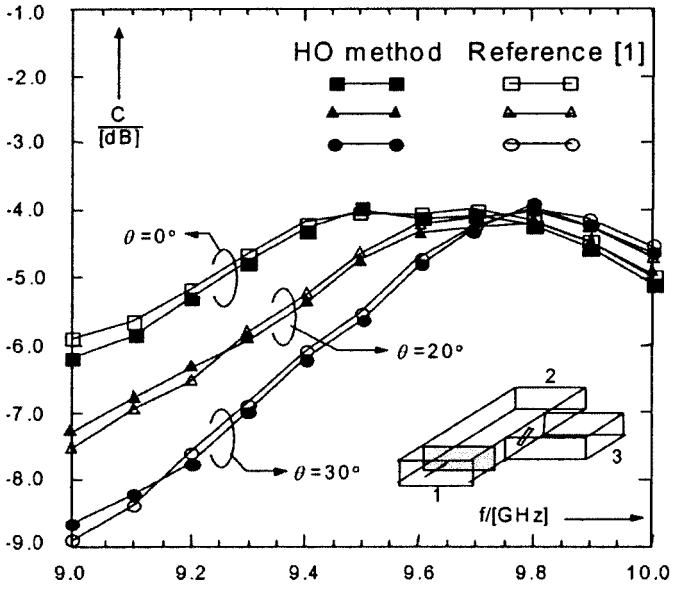

Fig. 4. Coupling coefficient of an inclined-slot coupled waveguide.

Next, a rectangular waveguide structure having the same format as that of Figs. 2 and 3, but with two perfectly conducting wedges of angle $\alpha = 5°$ is analyzed. Results of the relative error, are presented in Table I. Obviously, the proposed technique is equally efficient as in the degenerate case.

The coupling coefficient, C, of an inclined-slot junction (3-D structure) is, also, computed via the proposed technique. In Figs. 4 and 5 the coupling from port 1 to port 3 defined as

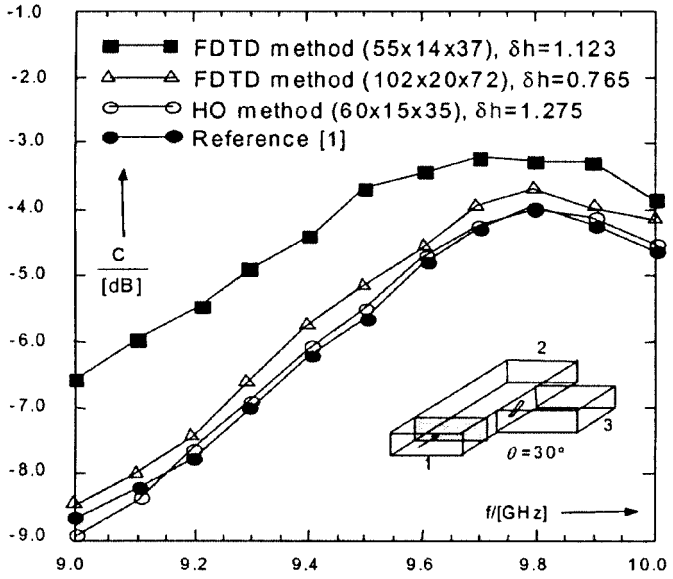

Fig. 5. Coupling coefficient of an inclined-slot coupled waveguide.

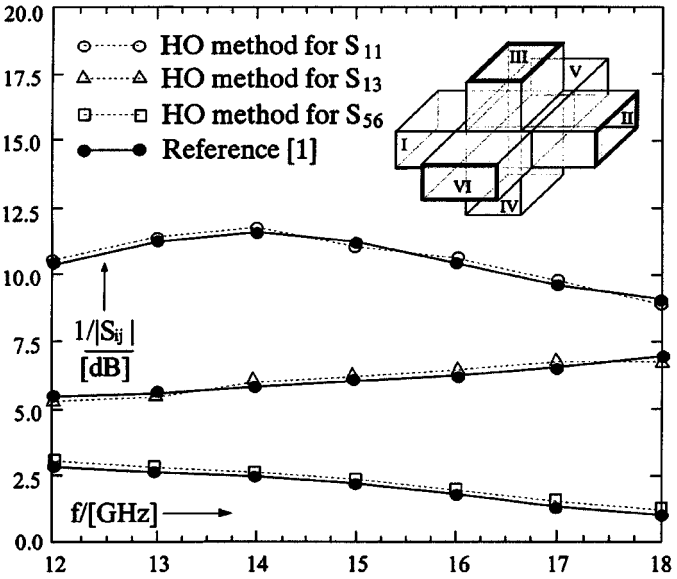

Fig. 6. The S-parameters of a six port junction.

$20\log|S_{13}|$ is demonstrated and compared to the results of [1]. The remarkable agreement for various inclinations of the slot and grid dimensions is obvious.

Additionally, the magnitude of various S-parameters of a six-port cross junction, $\alpha_1 = \alpha_2 = \alpha_3 = 15.799$ mm, $b_1 = b_2 = b_3 = 7.899$ mm) is illustrated in Fig. 6. Finally, the variation of S_{21}-parameter for a curvilinear iris-coupled resonator, is analyzed in Fig. 7. The promising accuracy and memory savings (almost 80% of Yee scheme) achieved by the HO FDTD scheme, are easily realized. The structures are, also, terminated by HO versions of existing PMLs [11], [12].

V. CONCLUSIONS

A novel methodology combining accurate higher-order curvilinear conventional and nonstandard FDTD concepts with a spatially-localized wavelet-based technique, has been

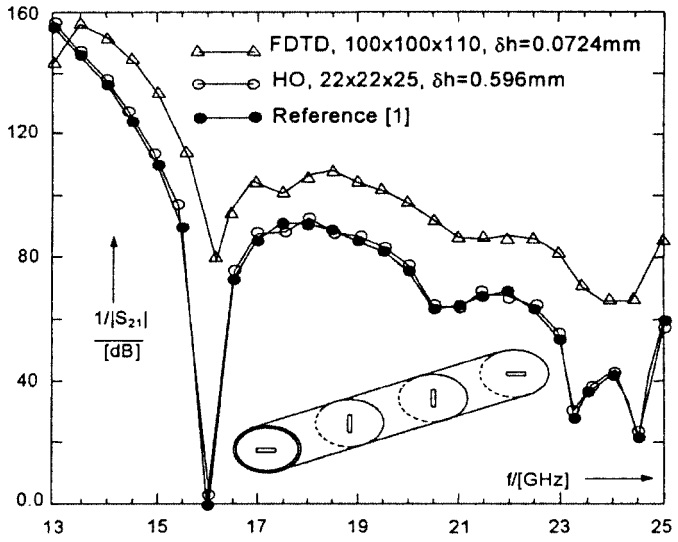

Fig. 7. The S_{21}-parameter of an iris-coupled resonator.

presented in this paper. Implementing the former at the nondiscontinuity regions and the latter close to singularities, the novel scheme has the ability to efficiently deal with waveguide discontinuity problems achieving high accuracy, significantly reduced dispersion errors and remarkable resource savings. Verification of the above merits is attained via numerical treatment of various complex waveguides.

REFERENCES

[1] A. Taflove, Ed., *Advances in Computational Electrodynamics: The Finite-Difference Time-Domain Method*. Boston: Artech House, 1998.

[2] S. Groiss, I. Bárdi, O. Bíró, K. Preis, and K. R. Richter, "A finite element analysis of multiport filters using perfectly matched layers," *IEEE Trans. Magn.*, vol. 33, no. 2, pp. 1480–1483, Mar. 1997.

[3] R. Schuhmann and T. Weiland, "Stability of the FDTD algorithm on nonorthogonal grids related to the spatial interpolation scheme," *IEEE Trans. Magn.*, vol. 34, no. 5, pp. 2751–2754, Sept. 1998.

[4] S. D. Gedney, F. S. Lansing, and D. Rascoe, "A full wave analysis of microwave monolithic circuit devices using a generalized Yee-algorithm based on an unstructured grid," *IEEE Trans. Microwave Theory Tech.*, vol. 44, no. 8, pp. 1393–1400, Aug. 1996.

[5] M. Fuji and W. J. R. Hoefer, "A three-dimensional Haar-wavelet-based multiresolution analysis similar to the FDTD method-derivation and application," *IEEE Trans. Microwave Theory Tech.*, vol. 46, no. 12, pp. 2463–2475, Dec. 1998.

[6] E. M. Tentzeris, R. L. Robertson, J. F. Harvey, and L. P. B. Katehi, "Stability and dispersion analysis of Battle–Lemarie-based MRTD schemes," *IEEE Trans. Microwave Theory Tech.*, vol. 47, no. 7, pp. 1004–1013, July 1999.

[7] J. Fang, "Time domain finite difference computation for Maxwell's equations," Ph.D. dissertation, University of California at Berkeley, CA, 1989.

[8] N. V. Kantartzis and T. D. Tsiboukis, "A higher-order FDTD technique for the implementation of enhanced dispersionless perfectly matched layers combined with efficient absorbing boundary conditions," *IEEE Trans. Magn.*, vol. 34, no. 5, pp. 2736–2739, Sept. 1998.

[9] T. I. Kosmanis, N. V. Kantartzis, and T. D. Tsiboukis, "A hybrid FDTD–Wavelet-Galerkin technique for the numerical analysis of field singularities inside waveguides," *IEEE Trans. Magn.*, vol. 36, no. 4, pp. 902–906, July 2000.

[10] I. Daubechies, *Ten Lectures on Wavelets*. Philadelphia, PA: SIAM Rev., 1992.

[11] J.-P. Berenger, "A perfectly matched layer for the absorption of electromagnetic waves," *J. Comput. Physics*, vol. 114, pp. 185–200, Oct. 1994.

[12] L. Zhao and A. C. Cangellaris, "A GT-PML: Generalized theory of perfectly matched layers and its application to the reflectionless truncation of finite-difference time-domain grids," *IEEE Trans. Microwave Theory Tech.*, vol. 44, no. 12, pp. 2555–2563, Dec. 1996.